Table 2. Probe sets commonly altered both at 12 weeks and 30 weeks

Probe Set ID	*P value*		Fold change		Gene Symbol	Chromosome	Gene Title
	12W	30W	12W	30W			
Down							
1433815_at	0.0008	0.0074	-2.24	-1.72	Jakmip1	5qB3 *	janus kinase and microtubule interacting protein 1
1448411_at	0.0008	0.0045	-2.10	-2.00	Wfs1	5qB3 *	Wolfram syndrome 1
1419744_at	0.0357	0.0424	-1.45	-1.44	H2-DMb2	17qB1	histocompatibility 2, class II, locus Mb2
1442241_at	0.0357	0.0424	-1.41	-1.49	Srpk2	5qA3 *	Serine/arginine-rich protein specific kinase 2
1425620_at	0.0157	0.0284	-1.39	-1.22	Tgfbr3	5qE5 *	transforming growth factor, beta receptor III
1418712_at	0.0274	0.0284	-1.36	-1.47	Cdc42ep5	7qA1	CDC42 effector protein (Rho GTPase binding) 5
1441317_x_at	0.0011	0.0045	-1.34	-1.71	Jakmip1	5qB3 *	janus kinase and microtubule interacting protein 1
1455197_at	0.0357	0.0424	-1.26	-1.29	Rnd1	15qF1	Rho family GTPase 1
Up							
1418148_at	0.0087	0.0074	2.03	1.68	Abhd1	5qB1*	abhydrolase domain containing 1
1431328_at	0.0046	0.0424	1.50	1.21	Ppp1cb	5qB1*	protein phosphatase 1, catalytic subunit, beta isoform
1459714_at	0.0157	0.0284	1.35	1.57	---	4qE1	---
1449425_at	0.0357	0.0074	1.28	1.28	Wnt2	6qA2	wingless-related MMTV integration site 2
1457532_at	0.0357	0.0185	1.27	1.35	Garnl1	12qC1	GTPase activating RANGAP domain-like 1
1416569_at	0.0274	0.0118	1.25	1.24	Actl6a	3qA3	actin-like 6A
1446406_at	0.0460	0.0424	1.24	1.20	Paqr8	1qA4	Progestin and adipoQ receptor family member VIII
1446815_at	0.0357	0.0424	1.23	1.29	Dph4	2qE3	DPH4 homolog (JJJ3, S. cerevisiae)
1456328_at	0.0460	0.0284	1.22	1.33	Bank1	3qG3	B-cell scaffold protein with ankyrin repeats 1

* The probe sets on the chromosome 5.

Table 3

Table 3. Validation study of gene expression using RT-PCR

Gene	Genotype	N	Average	SEM	*P value*	
12w						
cdc42ep5	WT	8	0.68	0.02		
	KO	8	0.63	0.02	0.088	+
Rnd1	WT	8	0.42	0.01		
	KO	8	0.39	0.02	0.070	+
Wnt2	WT	8	0.42	0.01		
	KO	8	0.44	0.02	0.227	
Garnl1	WT	8	15.30	0.37		
	KO	8	14.62	0.61	0.180	
32w						
cdc42ep5	WT	5	0.63	0.01		
	KO	7	0.66	0.03	0.225	
Rnd1	WT	5	0.58	0.04		
	KO	7	0.54	0.04	0.235	
Wnt2	WT	5	0.40	0.01		
	KO	7	0.44	0.02	0.041	*
Garnl1	WT	5	12.95	0.16		
	KO	7	14.37	0.64	0.049	*

The gene expression levels were normalized by Gapdh.
Each value represents the gene/Gapdh ratio x10-2.
P values were calculated by Mann-Whitney U-test (one tailed).
*: $P < 0.05$, +: $P < 0.10$

Supplementary Figure 1

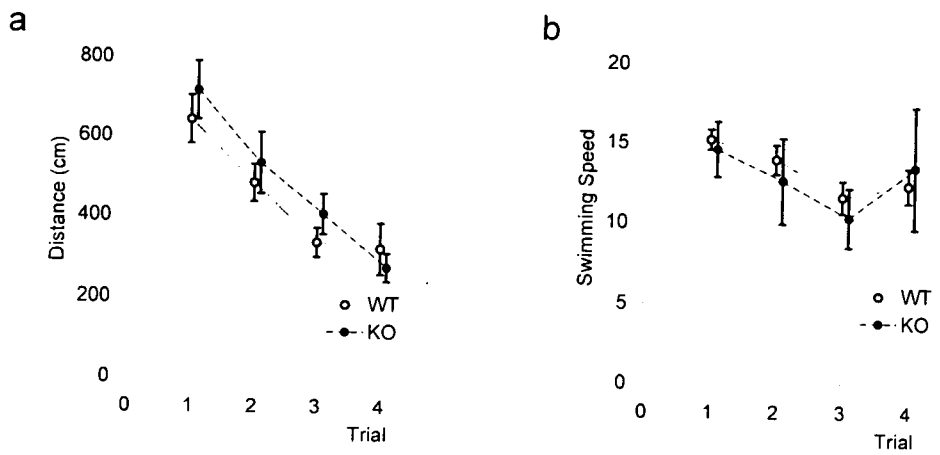

Supplementary Figure 1. Additional data of Morris water maze test.
a) Distance traveled. b) Swimming speed. Bars indicate standard errors.

Supplementary Table 1

Supplementary Table 1. Gene ontology analysis of differentially expressed genes at the age of 12 weeks

Category	Genes in Category	% of Genes in Category	Genes in List in Category	% of Genes in List in Category	*P* Value
GO:30529: ribonucleoprotein complex	641	3.20	41	7.48	0.000000451
GO:5737: cytoplasm	5472	27.28	201	36.68	0.000000711
*GO:3735: structural constituent of ribosome	409	1.94	30	5.12	0.00000146
GO:5840: ribosome	295	1.47	22	4.02	0.0000224
GO:5739: mitochondrion	1242	6.19	59	10.77	0.0000244
GO:6412: protein biosynthesis	892	4.56	44	8.02	0.000213
GO:9059: macromolecule biosynthesis	1001	5.12	47	8.56	0.000395
GO:43229: intracellular organelle	10184	50.78	316	57.66	0.000611
GO:43226: organelle	10184	50.78	316	57.66	0.000611
GO:5829: cytosol	478	2.38	26	4.75	0.000735
*GO:5622: intracellular	12285	61.25	370	67.52	0.00119
*GO:44249: cellular biosynthesis	1485	7.59	61	11.11	0.00172
GO:9058: biosynthesis	1727	8.83	69	12.57	0.00175
GO:43170: macromolecule metabolism	5573	28.48	187	34.06	0.00218
GO:43231: intracellular membrane-bound organelle	8934	44.54	276	50.36	0.00317
GO:43227: membrane-bound organelle	8934	44.54	276	50.36	0.00317
GO:19538: protein metabolism	3934	20.10	136	24.77	0.00394
GO:44260: cellular macromolecule metabolism	3939	20.13	136	24.77	0.00412
*GO:3723: RNA binding	931	4.41	40	6.83	0.00425
GO:15078: hydrogen ion transporter activity	181	0.86	12	2.05	0.00474
GO:15077: monovalent inorganic cation transporter activity	183	0.87	12	2.05	0.00517
GO:44267: cellular protein metabolism	3887	19.86	133	24.23	0.00631
*GO:7046: ribosome biogenesis	173	0.88	11	2.00	0.00979
GO:5743: mitochondrial inner membrane	254	1.27	14	2.56	0.0104
GO:43234: protein complex	2741	13.67	94	17.15	0.011
GO:5875: microtubule associated complex	183	0.91	11	2.01	0.0121
GO:5783: endoplasmic reticulum	803	4.00	33	6.02	0.0133
GO:42254: ribosome biogenesis and assembly	186	0.95	11	2.00	0.0161
GO:15630: microtubule cytoskeleton	465	2.32	21	3.83	0.0175
GO:19866: inner membrane	301	1.50	15	2.74	0.019
GO:5740: mitochondrial membrane	330	1.65	16	2.92	0.0198
GO:8380: RNA splicing	281	1.44	14	2.55	0.0279
GO:5198: structural molecule activity	1025	4.85	39	6.66	0.0289
*GO:15399: primary active transporter activity	232	1.10	12	2.05	0.029
*GO:5623: cell	17593	87.72	495	90.33	0.0311
GO:4386: helicase activity	183	0.87	10	1.71	0.0319
*GO:7028: cytoplasm organization and biogenesis	212	1.08	11	2.00	0.0374

Among 1012 probe sets (non-para, $P < 0.05$), 549 probe sets were used for GO analysis

* Shared with the GO at week 30.

Supplementary Table 2

Supplementary Table 2. Gene ontology analysis of differentially expressed genes at the age of 30 weeks

Category	Genes in Category	% of Genes in Category	Genes in List in Category	% of Genes in List in Category	*P* Value
GO:9142: nucleoside triphosphate biosynthesis	73	0.37	16	1.06	0.000117
GO:9145: purine nucleoside triphosphate biosynthesis	67	0.34	15	0.99	0.000147
GO:9206: purine ribonucleoside triphosphate biosynthesis	67	0.34	15	0.99	0.000147
GO:9201: ribonucleoside triphosphate biosynthesis	67	0.34	15	0.99	0.000147
GO:19904: protein domain specific binding	98	0.46	19	1.16	0.000171
GO:16043: cell organization and biogenesis	2692	13.76	254	16.78	0.000299
*GO:3723: RNA binding	931	4.41	100	6.09	0.000567
GO:9205: purine ribonucleoside triphosphate metabolism	76	0.39	15	0.99	0.000627
GO:9144: purine nucleoside triphosphate metabolism	79	0.40	15	0.99	0.000956
GO:9199: ribonucleoside triphosphate metabolism	79	0.40	15	0.99	0.000956
GO:166: nucleotide binding	3034	14.36	279	16.99	0.00106
GO:9141: nucleoside triphosphate metabolism	88	0.45	16	1.06	0.00107
GO:15405: P-P-bond-hydrolysis-driven transporter activity	132	0.63	21	1.28	0.00128
GO:6164: purine nucleotide biosynthesis	91	0.47	16	1.06	0.00155
GO:9152: purine ribonucleotide biosynthesis	84	0.43	15	0.99	0.00183
*GO:5623: cell	17593	87.72	1412	89.99	0.00193
GO:9260: ribonucleotide biosynthesis	93	0.48	16	1.06	0.00196
GO:5488: binding	14279	67.57	1162	70.77	0.00202
GO:6996: organelle organization and biogenesis	1443	7.37	141	9.31	0.00205
GO:902: cellular morphogenesis	521	2.66	58	3.83	0.00322
#GO:48666: neuron development	232	1.19	30	1.98	0.00384
GO:15662: ATPase activity, coupled to transmembrane movement of ions, phosphorylative mechanism	91	0.43	15	0.91	0.00424
GO:6754: ATP biosynthesis	50	0.26	10	0.66	0.0044
GO:6753: nucleoside phosphate metabolism	50	0.26	10	0.66	0.0044
GO:6812: cation transport	610	3.12	65	4.29	0.00526
GO:42625: ATPase activity, coupled to transmembrane movement of ions	102	0.48	16	0.97	0.00529
GO:3676: nucleic acid binding	4886	23.12	422	25.70	0.00576
GO:45892: negative regulation of transcription, DNA-dependent	150	0.77	21	1.39	0.0058
#GO:30182: neuron differentiation	282	1.44	34	2.25	0.00661
GO:6818: hydrogen transport	96	0.49	15	0.99	0.00676
GO:3743: translation initiation factor activity	124	0.59	18	1.10	0.00735
GO:9150: purine ribonucleotide metabolism	97	0.50	15	0.99	0.00744
GO:6916: anti-apoptosis	125	0.64	18	1.19	0.00763
GO:5856: cytoskeleton	1308	6.52	126	8.03	0.00801
GO:48468: cell development	349	1.78	40	2.64	0.00809
GO:8135: translation factor activity, nucleic acid binding	184	0.87	24	1.46	0.00859
GO:6163: purine nucleotide metabolism	109	0.56	16	1.06	0.00959
GO:43492: ATPase activity, coupled to movement of substances	118	0.56	17	1.04	0.0097
GO:42626: ATPase activity, coupled to transmembrane movement of substances	118	0.56	17	1.04	0.0097
GO:19901: protein kinase binding	64	0.30	11	0.67	0.00977
GO:9165: nucleotide biosynthesis	167	0.85	22	1.45	0.0098
GO:6413: translational initiation	91	0.47	14	0.93	0.00995
GO:45182: translation regulator activity	197	0.93	25	1.52	0.0104
GO:16820: hydrolase activity, acting on acid anhydrides, catalyzing transmembrane movement of substances	119	0.56	17	1.04	0.0105
GO:15992: proton transport	83	0.42	13	0.86	0.011
GO:16887: ATPase activity	260	1.23	31	1.89	0.0114

GO:904: cellular morphogenesis during differentiation	220	1.12	27	1.78	0.0115
GO:9259: ribonucleotide metabolism	112	0.57	16	1.06	0.0123
#GO:7409: axonogenesis	161	0.82	21	1.39	0.0127
GO:7015: actin filament organization	67	0.34	11	0.73	0.0132
GO:7010: cytoskeleton organization and biogenesis	717	3.66	72	4.76	0.0134
GO:50877: neurophysiological process	372	1.90	41	2.71	0.0139
GO:46034: ATP metabolism	59	0.30	10	0.66	0.0143
GO:17111: nucleoside-triphosphatase activity	410	1.94	44	2.68	0.0183
GO:19900: kinase binding	70	0.33	11	0.67	0.0186
GO:9892: negative regulation of metabolism	326	1.67	36	2.38	0.0196
*GO:5622: intracellular	12285	61.25	999	63.67	0.0212
GO:19001: guanyl nucleotide binding	571	2.70	58	3.53	0.0217
GO:6811: ion transport	885	4.52	85	5.61	0.0219
GO:122: negative regulation of transcription from RNA polymerase II promoter	91	0.47	13	0.86	0.0226
*GO:15399: primary active transporter activity	232	1.10	27	1.64	0.0229
*GO:7028: cytoplasm organization and biogenesis	212	1.08	25	1.65	0.023
GO:5525: GTP binding	563	2.66	57	3.47	0.024
GO:7275: development	2749	14.05	239	15.79	0.0246
*GO:7046: ribosome biogenesis	173	0.88	21	1.39	0.0265
GO:6605: protein targeting	301	1.54	33	2.18	0.0269
GO:3674: molecular_function	20838	98.61	1628	99.15	0.0275
#GO:7399: nervous system development	675	3.45	66	4.36	0.0287
#GO:48667: neuron morphogenesis during differentiation	196	1.00	23	1.52	0.0297
#GO:31175: neurite morphogenesis	196	1.00	23	1.52	0.0297
GO:15031: protein transport	981	5.01	92	6.08	0.0303
GO:8092: cytoskeletal protein binding	584	2.76	58	3.53	0.032
*GO:44249: cellular biosynthesis	1485	7.59	134	8.85	0.032
GO:19226: transmission of nerve impulse	262	1.34	29	1.92	0.0325
GO:42802: protein self binding	187	0.89	22	1.34	0.0335
GO:5515: protein binding	5994	28.36	498	30.33	0.0357
GO:48519: negative regulation of biological process	906	4.63	85	5.61	0.0359
GO:16481: negative regulation of transcription	243	1.24	27	1.78	0.0365
GO:16818: hydrolase activity, acting on acid anhydrides, in phosphorus-containing anhydrides	441	2.09	45	2.74	0.0368
GO:9889: regulation of biosynthesis	169	0.86	20	1.32	0.0375
GO:16817: hydrolase activity, acting on acid anhydrides	442	2.09	45	2.74	0.038
GO:5085: guanyl-nucleotide exchange factor activity	179	0.85	21	1.28	0.0381
GO:1654: eye development	69	0.35	10	0.66	0.0388
*GO:3735: structural constituent of ribosome	409	1.94	42	2.56	0.0389
GO:15672: monovalent inorganic cation transport	366	1.87	38	2.51	0.0391
GO:17076: purine nucleotide binding	2795	13.23	241	14.68	0.0398
GO:3779: actin binding	410	1.94	42	2.56	0.0402
GO:7017: microtubule-based process	313	1.60	33	2.18	0.0432
GO:6457: protein folding	269	1.38	29	1.92	0.0435
GO:45184: establishment of protein localization	1010	5.16	93	6.14	0.0437
GO:42803: protein homodimerization activity	100	0.47	13	0.79	0.0458
GO:16462: pyrophosphatase activity	437	2.07	44	2.68	0.0463
GO:7600: sensory perception	121	0.62	15	0.99	0.0467
GO:9653: morphogenesis	1076	5.50	98	6.47	0.0495
GO:48731: system development	720	3.68	68	4.49	0.0498

Among 3508 probe sets (non-para, $P < 0.05$), 1514 probe sets were used for GO analysis

* Shared with the GO at week 30.

GO related to neural development

 Articles in PresS. Am J Physiol Endocrinol Metab (January 29, 2008). doi:10.1152/ajpendo.00640.2007

REVISED manuscript/E-00640-2007R1

Ambient Glucose Levels Qualify the Potency of Insulin Myogenic Actions by Regulating SIRT1 and FoxO3a in C2C12 myocytes

Taku Nedachi[1], Akito Kadotani[1,3], Miyako Ariga[1,2], Hideki Katagiri[2,3] and Makoto Kanzaki[1,4*]

[1]Division of Biomaterials, Tohoku University Biomedical Engineering Research Organization (TUBERO), [2]21st COE program "CRESCENDO", Graduate School of Pharmaceutical Sciences, [3]Division of Advanced Therapeutics for Metabolic Diseases, Center for Translational and Advanced Animal Research, [4]Center for Research Strategy and Support (CRESS), Tohoku University, Sendai 980-8575, Japan

Running Title: SIRT1 and FoxO3a in differentiating C2C12 myocytes

*To whom correspondence should be addressed: Center for Research Strategy and Support (CRESS), Tohoku University, 2-1 Seiryo-machi, Aoba-ku, Sendai 980-8575, JAPAN, Tel: +81-22-717-7581; Fax: +81-22-717-7578; E-mail: Kanzaki@tubero.tohoku.ac.jp

ABSTRACT

Nutrition availability is one of the major environmental signals influencing cell fates such as proliferation, differentiation and apoptosis, often functioning in concert with other humoral factors including insulin. Herein, we show that low serum-induced differentiation of C2C12 myocytes is significantly hampered under low glucose (LG: 5 mM glucose) as compared with high glucose (HG: 22.5 mM glucose) conditions, concurrently with nuclear accumulation of SIRT1, an NAD^+-dependent deacetylase, and FoxO3a, both of which are implicated in the negative regulation of myogenesis. Intriguingly, insulin appears to exert opposite actions, depending upon glucose availability, in regard to the regulation of SIRT1 and FoxO3a abundance, which apparently contributes to modulating the potency of insulin's myogenic action. Namely, insulin exerts a potent myogenic effect in the presence of sufficient glucose, while insulin is unable to exert its myogenic action under LG conditions, since insulin evokes massive up-regulation of both SIRT1 and FoxO3a in the absence of sufficient ambient glucose. In addition, the hampered differentiation state under LG is significantly restored by sirtinol, a SIRT1 inhibitor, whereas insulin abolished this sirtinol-dependent restoration, indicating that insulin can function as a negative, as well as a positive, myogenic factor depending upon glucose availability. Taken together, our data reveal the importance of ambient glucose levels in the regulation of myogenesis and also in the determination of insulin's myogenic potency, which is achieved at least in part through regulation of the cellular contents and localization of SIRT1 and FoxO3a in differentiating C2C12 myocytes.

INTRODUCTION

Skeletal muscle cells have provided a useful model for exploring the molecular mechanisms involved in cellular differentiation (13), and insulin and insulin-like growth factors (IGFs) have been implicated in the process of myogenesis by activating the IRS-PI3 kinase signaling pathway (7, 22, 25, 53) that also serves as a pivotal intracellular signal for exerting metabolic actions in mature skeletal muscle (9). However, despite our general understanding of the effects of ambient glucose levels on insulin-responsiveness with regard to metabolic actions in skeletal muscle cells (37), the possible interrelationship between glucose and insulin acting on myogenesis remains to be clarified.

Skeletal muscle differentiation is a well-organized process governed by muscle-specific transcription factors belonging to the MyoD family, such as MyoD and myogenin, (42), and the myocyte enhancer factor 2 (MEF2) family, such as MEF2A and MEF2C (35). In addition to these muscle-specific transcription factors, positively regulating myogenesis, the Forkhead box O (FoxO) class of transcription factors, ubiquitously expressed in various cell types, has been shown to negatively regulate myogenesis (27). Insulin/IGF-induced repression of FoxO transcription factors, resulting from their nuclear exclusion in response to Akt-mediated phosphorylation, has been implicated in a key aspect of insulin/IGF actions not only for stimulating myogenesis but also for preventing muscle atrophy (21, 46).

Myogenesis is also directly influenced by the acetylation status of histones and non-histone proteins including MyoD and MEF2, and Class I and II histone deacetylases (HDACs) have been shown to regulate muscle gene expression by inhibiting MyoD and MEF2 factors (31, 33, 43). Recently, Silent information

regulator-2 (Sir2), a class III deacetylase originally characterized as controlling the life spans of animals in response to nutritional availability, was also identified to serve as a key regulator for myogenesis (14) *via* overexpression of SIRT1, the mammalian ortholog for Sir2, in C2C12 myoblasts by strongly inhibiting differentiation into myotubes, whereas suppression of SIRT1 expression by RNA interference enhanced myogenesis (14).

Given the unique property of SIRT1 that the cofactor nicotinamide adenine dinucleotide (NAD^+) drives deacetylation activity, SIRT1 has been thought to serve as an energy and/or oxidation sensor, being directly involved in the nutritional regulation of gene transcription events in various tissues including skeletal muscle (38, 40, 45). Intriguingly, recent studies have also demonstrated that SIRT1 controls cellular functions by deacetylating FoxO transcription factors in response to various stimuli including nutritional availability (4, 36, 38). Thus, myogenesis is likely to be regulated cooperatively by SIRT1 serving as a sensor of the nutritional environment in concert with FoxOs serving as an insulin/IGF sensor in various situations in which glucose and insulin levels are fluctuating. However, no data are available on the potential interplay between ambient glucose levels and insulin in the regulations of SIRT1 and FoxOs, or on the regulation of myogenesis.

In order to gain insight into these issues, we investigated the effects of ambient glucose levels on differentiation of C2C12 myocytes, and found the potency of insulin's myogenic action to be remarkably affected by extracellular glucose levels, and that insulin exerts its maximum myogenic effect only in the presence of a relatively high level of glucose, while its potency is significantly compromised under low glucose (LG) conditions, a state in which massive up-regulations of SIRT1 and FoxO3a are induced

by insulin treatment. Thus, these findings reveal an important interplay between ambient glucose and insulin favoring alterations in the cellular contents of SIRT1 and FoxO3a, both of which are tightly coupled to the regulation of myogenesis.

MATERIALS AND METHODS

Materials - The Western blot detection kit (West super femto detection reagents) was obtained from Pierce Biotechnology Inc. (Rockford, IL, USA). Dulbecco's Modified Eagle Medium (DMEM), penicillin/streptomycin and Trypsin-EDTA were purchased from Sigma Chemicals (St. Louis, MO, USA). Cell culture equipment was from BD Biosciences (San Jose, CA, USA). Calf Serum (CS) and Fetal Bovine Serum (FBS) were obtained from BioWest (Nuaille, France). Immobilon-P and anti-SIRT1 antibody were from Millipore Corp. (Bedford, MA, USA). Anti-myosin heavy chain (MHC) (MF20) and anti-myogenin (F5D) antibodies were obtained from Iowa Hybridoma Bank (University of Iowa, Iowa City, IA, USA). Anti-phospho S6 (Ser235/236), anti-Akt, anti-phospho Akt (Ser473), anti-phospho Akt (Thr308) antibodies were purchased from Cell Signaling Technology Inc. (Danvers, MA, USA). Anti-β-actin antibody was obtained from Sigma Chemicals. Unless otherwise noted, all chemicals were of the purest grade available from Sigma Chemicals.

Cell Culture - Mouse skeletal muscle cell lines, C2C12 myoblasts (54), were maintained in DMEM supplemented with 10% FBS, 30 μg/ml penicillin, and 100 μg/ml streptomycin (growth medium) at 37°C under a 5% CO_2 atmosphere. For biochemical study, the cells were grown on 4-well plates (Nalgen Nunc International, Rochester, NY, USA) at a density of 1 x 10^5 cells/well in 5 ml of growth medium or on 6 well plates (BD Biosciences) at a density of 3 x 10^4 cells/well in 3 ml of growth medium. Three days after plating, cells had reached approximately 80-90% confluence (*Day 0*). Differentiation was then induced by switching the growth medium to DMEM supplemented with 2% CS, 30 μg/ml penicillin and 100 μg/ml streptomycin

(differentiation medium). The differentiation medium was changed every 24 hours. For the immunofluorescent staining study, cells were grown on 22-mm glass coverslips (Matsunami C022221, Osaka, Japan) in 6-well plates.

Immunofluorescent studies - C2C12 were cultured on cover slips placed on 6-well plates. After differentiation, the cells were stimulated with 100 nM insulin for 60 min. Then, the cells were fixed with 2% paraformaldehyde in PBS (-), followed by immunocytochemistry using anti-SIRT1 antibody (Millipore Corp), and anti-mouse IgG antibody conjugated with Alexa 555 or Alexa 594 (Invitrogen Corp., Carlsbad, CA, USA). Images were monitored and analyzed using Olympus Fluoview FV1000 confocal microscopy and the associated application program, ASW Ver1.3 (Olympus, Tokyo Japan).

Nuclear extract preparation – Nuclear extract preparation was performed as follows. Briefly, the cells were washed three times with PBS (-), and re-suspended in buffer A (10 mM HEPES-OH (pH 7.9), 1.5 mM $MgCl_2$, 10 mM KCl). After a 20 minute incubation on ice, the cells were destroyed with a vortex mixer (maximum speed), and the pellets were then collected. The pellets were re-suspended in 50 μl of Buffer C (HEPES-OH (pH 7.9), 420 mM NaCl, 1.5 mM $MgCl_2$, 0.2 mM EDTA, 25% Glycerol), then frozen (-80 °C) and thawed twice. The supernatants were collected as nuclear extracts, the protein concentration was measured, and then stored at -80 °C until Western blot analysis.

Immunoprecipitation – The cell lysates were prepared using Triton X-100/NP40 lysis

buffer (50 mM Tris-Cl, 150 mM NaCl, 1 mM EDTA, 1% Triton X-100, 1% NP-40) and the protein concentrations of each sample were measured using a BCA protein assay kit (PIERCE). Five hundred μg of protein were mixed with 2 μg of anti-SIRT1 polyclonal antibody. The mixtures were incubated at 4 °C for 3 hours, and continuously incubated in the presence of protein A-sepharose. The immunoprecipitates were washed with Triton X-100/NP-40 lysis buffer three times. The adsorbed proteins were eluted with 1 x Laemmli's buffer, boiled, and subjected to Western blot analysis.

Western blot analysis - The expression and phosphorylation of each protein were analyzed by western blot analysis. In brief, the harvested cell lysates were subjected to 5% or 12% SDS-polyacrylamide gel electrophoresis (1: 30 bis: acrylamide). Proteins were transferred to a PVDF membrane (Immobilon-P: Millipore Corp), and the membranes were then blocked for 2 hours at room temperature with 5% non-fat dry milk in Tris buffered saline (TBS) containing 0.1% Tween 20. Immunostaining to detect each protein was achieved with a 1 h incubation with a 1:1000 dilution of anti-SIRT1 antibody, anti-myosin heavy chain antibody and anti-myogenin antibody. Specific total or phospho-proteins were visualized after subsequent incubation with a 1:5000 dilution of anti-mouse or rabbit IgG conjugated to horseradish peroxidase and a SuperSignal Chemiluminescence detection procedure (Pierce Biotechnology Inc.). Protein concentrations were determined using a bicinchoninic acid assay (BCA) (Pierce Biotech. Inc). Three independent experiments were performed for each condition. Coomassie blue staining was also performed to assess the efficiency of protein transfer.

Real Time PCR - Fluorescence real time PCR analysis was performed using a Light

Cycler instrument and SYBR Green detection kit according to the manufacturer's instructions (Roche Diagnostics Corporation, Indianapolis, IN, USA). PCR primers for measuring each of the secreted factors were as follows (for SIRT1: 5'-GAT CCT TCA GTG TCA TGG TT-3' and 5'-GAA GAC AAT CTC TGG CTT CA-3'; for FoxO3a: 5'-TGC CTT GTC AAA TTC TGT C-3' and 5'-TGC ACT AGC TGA ATA CAG TGA G-3'; for GAPDH: 5'-GGA GAA ACC TGC CAA GTA TGA-3' and 5'-GCA TCG AAG GTG GAA GAG T-3').

Glucose Concentration Assay - Glucose concentrations in the cultured media were measured using a determiner GLE kit (Kyowa Medex, Tokyo, Japan)

Statistical Analysis - Statistical analysis was performed using one-way ANOVA followed by Tukey's multiple comparison test or Student's paired t test for independent samples. Data are expressed as means +/- SEM unless otherwise specified.

RESULTS

Extracellular glucose influences low-serum induced C2C12 differentiation

To characterize the effects of extracellular glucose levels on myogenesis of C2C12 cells, we first examined whether the glucose concentration in the low-serum differentiation medium (D-MEM + 2% calf serum) affects C2C12 differentiation. Under the LG (5 mM glucose) conditions, the process of myogenesis was obviously delayed and the number of well-developed myotubes was decreased as compared to high glucose (22.5 mM glucose; HG) conditions on *Day 4* of differentiation (Fig. 1A). We quantified differentiation status by counting the number of myotubes defined as multinuclear myotubes which contained more than 5 nuclei (Fig. 1B), as we previously reported (37). The effect of the extracellular glucose concentration on myogenesis was confirmed by western blot analysis of differentiation marker proteins using anti-skeletal muscle type myosin heavy chain (MHC) and anti-myogenin antibodies as not only were their expressions detected later, but their amounts were also lower than in C2C12 cells differentiated under LG conditions (Fig. 1C).

SIRT1 predominantly localizes in the nucleus under LG conditions, but is excluded under HG conditions in C2C12 myotubes

To understand the mechanisms by which extracellular glucose alters the process of C2C12 differentiation, we initially focused on SIRT1, a NAD-dependent protein deacetylase with enzymatic activity sensitive to changes in cellular energy levels (for a review, see Ref. (2)), since a recent study showed direct involvement of SIRT1 in myogenesis (14). Consistent with previous reports showing that Sir2 and its mammalian homologue SIRT1 are localized in the nucleus (19, 34), immunofluorescent analysis

using anti-SIRT1 antibody demonstrated that when C2C12 cells were differentiated under LG conditions, predominant localization of SIRT1 was observed in the nucleus (Fig. 2A, *panel a*) similar to what was observed in undifferentiated myoblasts (data not shown). In contrast, when C2C12 myoblasts were differentiated under HG conditions, the number of SIRT1-positive nuclei was remarkably reduced (Fig. 2A: *panel c, see arrowheads*), as confirmed by western blotting analysis of nuclear proteins extracted under each culture condition (data not shown). Counterstaining was performed with DAPI (*panels b* and *d*). Immunofluorescent analysis demonstrated that the nuclear exclusion of SIRT1 was not acutely induced by HG administration in either myoblasts (data not shown) or LG-differentiated myotubes (Figure 2B). However, we found that total SIRT1 protein was significantly reduced when C2C12 cells were differentiated under HG conditions (Fig. 2C, *lower panel, HG-SIRT1*) as compared to those under LG conditions (*upper panel, LG-SIRT1*). The HG-dependent reduction of SIRT1 was obvious from *Day 2* of differentiation (Fig. 2C, *lower panel, HG-SIRT1, lane3*).

Myogenesis is a highly organized and regulated sequence of multiple processes orchestrated by a wide variety of functional proteins including SIRT1, requiring a relatively long time, and all of these processes could be affected by ambient glucose levels. In an attempt to dissect the effects of glucose on SIRT1 regulation and myogenesis, we conducted an experiment to specify the time required for glucose to exert its effect on SIRT1 suppression. Thus, C2C12 myotubes differentiated under LG conditions (*days 5-6*) were transferred to HG or the same LG medium, and time-course changes in SIRT1 contents were analyzed by western blotting (Fig. 2D and 2E). The time-course experiment revealed that 24 h exposure to HG is sufficient for reducing the cellular SIRT1 content and its nuclear localization (data not shown) in LG-differentiated

C2C12 myotubes. In addition, we performed the converse experiments, that is, C2C12 myotubes were cultured under HG conditions, then switched to LG for the indicated time to confirm that amounts of SIRT1 were reversibly controlled by ambient glucose levels (Fig. 2F). We also measured SIRT1 mRNA levels under these conditions, and found that SIRT1 mRNA was significantly induced by switching to the LG condition ($p<0.05$, $n=4$) (Fig. 2G). Thus, these results suggest that SIRT1 protein induction is regulated, at least in a part, by its mRNA levels.

Foxo3a predominantly localizes in the nucleus under LG conditions, but is excluded under HG conditions in C2C12 myotubes

We next examined whether FoxO3a associates with the spatio-temporal changes in SIRT1 localization in response to alterations in glucose availability, since recent reports revealed functional and physical interactions between SIRT1 and FoxO transcription factors in response to various stimuli including oxidative stress (4, 36) and nutritional circumstances (38). Similar to the pattern observed in SIRT1 subcellular localization, FoxO3a was predominantly detected in the nuclei of myotubes when the cells were differentiated under LG conditions (Fig. 3A, *panel a*), while no nuclear localization of FoxO3 was observed in those differentiated under HG conditions (Fig 3A, *panel c*). Again, HG administration failed to induce acute redistribution of FoxO3a (Fig. 3B), but resulted in a remarkable reduction of FoxO3a when the LG-differentiated myotubes (*Day 5-6*) were exposed to HG for an additional 24 h (Fig. 3D and 3E). Furthermore, we confirmed that FoxO3a protein was reversibly controlled by extracellular glucose (Fig. 3F) and also that FoxO3a mRNA levels were regulated by extracellular glucose ($p<0.001$, $n=4$) (Fig. 3G). Thus, FoxO3a displayed

spatio-temporal regulation similar to that observed in SIRT1 in response to altered extracellular glucose levels. However, the changes in cellular FoxO3a content during myogenesis were obviously different from those of SIRT1. As shown in Fig 3C, little FoxO3a expression was observed in undifferentiated myoblasts (*Day 0*), but its expression gradually increased upon differentiation only under LG conditions. This differentiation-dependent increase in the cellular content of FoxO3a was abolished when the cells were differentiated under HG conditions.

Taken together, these data demonstrate that although acute HG treatment fails to induce subcellular redistributions of SIRT1 and FoxO3a, with chronic HG treatment (24h) there is an obvious nuclear exclusion of these proteins concomitant with the significant reductions in their cellular contents in differentiating C2C12 cells. These data also suggest the compromised myogenesis under LG conditions to be attributable to nuclear accumulation of relatively high levels of SIRT1 and FoxO3a in C2C12 cells. In addition, our data indicate that 24 h exposure to HG is sufficient to produce obvious reductions in both SIRT1 and FoxO3a proteins in C2C12 myotubes.

Extracellular glucose levels modify the stimulatory effect of insulin on myogenesis by altering cellular contents of SIRT1 and FoxO3a

Effects of HG appeared to be elicited within 24 h as assessed by the obvious reductions of both SIRT1 and FoxO3a proteins in the LG-differentiated C2C12 myotubes (Fig. 2 and 3). We therefore took advantage of this phenomenon to explore the possible interplay between insulin and ambient glucose during the regulation of myogenesis. Namely, the LG-differentiated C2C12 myotubes (*day 5-6*) were transferred to LG or HG medium in the absence or presence of the indicated insulin concentration

and cultured for an additional 24 h, and the cellular contents of SIRT1 and FoxO3a were then analyzed by western blotting (Fig. 4). In the presence of LG, insulin significantly increased cellular contents of both SIRT1 (Fig. 4A, *upper panel, lanes 1~6*) and FoxO3a (*middle panel, lanes 1~6*) in a dose-dependent manner (Fig. 4B and 4C, *open symbols*) although the amount of β-actin as a loading control was not changed (Fig. 4A, *lower panel*). In the presence of insulin under LG conditions for 24 h, SIRT1 predominantly displayed nuclear localization, while increased FoxO3a displayed both cytoplasmic and nuclear localization (data not shown). In sharp contrast, insulin treatment tended to decrease SIRT1 protein in the presence of HG (Fig. 4A, *upper panel, lanes 7~12,* Fig 4B, *closed circles*). Moreover, insulin completely failed to increase FoxO3a contents in the presence of HG (Fig. 4A, *lower panel, lanes 7~12*) (Fig. 4C, *closed triangles*). In the presence of insulin under HG conditions for 24 h, both these proteins were barely detectable by immunofluorescent staining (data not shown).

To address the possibility that these changes in SIRT1 and FoxO3a proteins induced by the combined actions of insulin and glucose contribute to regulating the differentiation status of C2C12 myotubes, the amount of MHC as a myogenic differentiation marker under each condition was also analyzed by western blotting (Fig. 5). Consistent with the results depicted in Fig. 1, the stimulatory effect of HG on MHC expression was also detected even after incubation for just 24 h with HG (Fig. 5A, *lane 1 vs. lane 6*). In the presence of HG, insulin displayed a potent myogenic stimulating action, and MHC amounts were significantly increased in response to 100 nM insulin ($p<0.05$, $n=3$) (Fig. 5A, *lanes 6~10*) under conditions in which the SIRT1 and FoxO3a contents were marginal (Fig. 4). In contrast, the myogenic stimulating potency of insulin was apparently limited (Fig 5A, *lanes 1~5*) under LG conditions in which